

ภาคผนวก ก

Manuscript สำหรับส่ง SONGKLANAKARIN (Journal of Science and Technology)

**Morphological Control and Optical Properties of Nanocrystalline ZnO Powder
from Precipitation Method**

S. Suwanboon¹, S. Chukamnerd² and U. Anglong²

Abstract

S. Suwanboon¹, S. Chukamnerd² and U. Anglong²

**Morphological Control and Optical Properties of Nanocrystalline ZnO Powder
from Precipitation Method**

Nanocrystalline ZnO powders have been synthesized by using zinc acetate dihydrate and PVP as starting materials. The calcined powders in air at 600 °C for 1 hour have been characterized by XRD, indexing the wurtzite or hexagonal structure with the smallest crystallite size of ~ 44.76 nm, and lattice parameters a and c of 0.3249 and 0.5204 nm, respectively at 3×10^{-4} M PVP. The SEM images show that the morphology has been changed from plate-like to small rod shape when adding PVP to solutions and the morphology has tended to be monosized at higher PVP concentration. The smallest grain sizes of ZnO powders are ~ 130 nm at 3×10^{-4} M PVP. The optical band gap of all ZnO powders in this study varied between 3.218-3.229 eV.

Key words : zinc oxide, PVP, precipitation

¹Ph.D. (Materials Chemistry), Material Science Program, Faculty of Science, Prince of Songkla University, Hat Yai, Songkhla 90112, Thailand.

E-mail address : ssumetha@yahoo.com

²Undergraduate Student, Material Science Program, Faculty of Science, Prince of Songkla University, Hat Yai, Songkhla 90112, Thailand.

Recently, nanocrystalline powder with uniform size and shape has shown interesting properties, particularly nanocrystalline metal oxides, due to its numerous important properties such as catalytic, electrical and optical properties as well as the nanocrystalline powders showed the distinguishable difference in these properties from macroscopic, microscopic and bulk materials (Cao, 2004). Among them, ZnO is one of the candidates that has been attracting attention because of its wide band gap energy of about 3.37 eV, and large exciton binding energy of 60 meV at room temperature. ZnO is thus important material for room temperature UV lasers and short-wavelength optoelectronic devices (Bao *et al.*, 1998; Majumder *et al.*, 2003). Furthermore, ZnO with its good electrical and optical properties, can be used in many applications such as photoconductors, integrated sensors and transparent conducting oxide electrodes (Huang *et al.*, 2003; Xu *et al.*, 2000). Nanocrystalline ZnO powders have been for use in piezoelectric sensors (Lee *et al.*, 2003), gas sensors (Patil *et al.*, 2007) and solar cell applications (Lee *et al.*, 2007).

Up to now, many soft chemical methods have been used to fabricate nanocrystalline ZnO powder, such as hydrothermal (Pal *et al.*, 2006), spray pyrolysis (Mohammad *et al.*, 2006) and precipitation or sol-gel (Tang *et al.*, 2006) methods. The sol-gel method shows many advantages over the other techniques, such as its simplicity and low equipment cost. Therefore, in this study we concentrated on evaluating the effect of PVP-capping agent to control the morphology and optical properties of ZnO powder prepared using the precipitation or sol-gel method in aqueous solution. At the present, there are a few reports focusing on the role of PVP (molecular weight of 40,000) in controlling the morphological ZnO powder. Therefore, in this study, we used PVP as capping agent because PVP dissolves very

well in many organic solvents. PVP can control the growth of inorganic crystal and it is inexpensive reagent (Yinghin et al., 2006)

Materials and Methods

All the chemical reagents used in this experiment were analytical grade and were used without further purification. In a typical procedure, 2.1949 g $\text{Zn}(\text{CH}_3\text{COO})_2 \cdot 2\text{H}_2\text{O}$ was first dissolved in 50 mL distilled water with continuous stirring until a homogeneous solution was obtained. Various amounts of polyvinylpyrrolidone (PVP, M.W. 40,000) were then added into previous zinc precursor solutions so as to investigate the role of PVP to control the shape and size of ZnO powders. Finally, 1.6 g NaOH that was dissolved in 50 mL distilled water was slowly added to the PVP-modified zinc precursor solution. The white precipitates were achieved and were then vigorously stirred at ambient temperature for 1 hour before filtering, rinsing with distilled water, drying at 60 °C and calcining at 600 °C for 1 hour.

The phase identifications of the calcined powders were examined by powder X-ray diffractometer (XRD, X'Pert MPD, Philips) with $\text{CuK}\alpha$ radiation ($\lambda = 0.15406$ nm). The shape and grain size of the calcined powders were evaluated with scanning electron microscopy (SEM, JSM-5800 LV, JOEL) and the optical spectra were measured in the range of 200-800 nm with a UV-VIS spectrophotometer (UV-2401, Shimadzu).

Results and Discussions

Structural properties

Influence of $\text{Zn}(\text{CH}_3\text{COO})_2 \cdot 2\text{H}_2\text{O}$ concentration

Figure 1 shows XRD patterns of calcined powders that were precipitated from 0.1 M and 0.2 M $\text{Zn}(\text{CH}_3\text{COO})_2 \cdot 2\text{H}_2\text{O}$. These peaks were indexed as the ZnO wurtzite structure in correspondence with JCPDS (card number 36-1451). The lattice parameters, a and c that were calculated from XRD peaks of ZnO powder prepared from 0.1 M $\text{Zn}(\text{CH}_3\text{COO})_2 \cdot 2\text{H}_2\text{O}$ were 0.3249 nm and 0.5204 nm, whereas the lattice parameters, a and c of ZnO powder prepared from 0.2 M $\text{Zn}(\text{CH}_3\text{COO})_2 \cdot 2\text{H}_2\text{O}$ were 0.3248 nm and 0.5206 nm, respectively. These lattice parameters of both ZnO powders are basically the same and close to the ZnO standard ($a = 0.3250$ nm and $c = 0.5206$ nm). The crystallite sizes of both ZnO powders, estimated from X-ray line broadening using Scherrer's equation, were ~ 40 nm (Mahuya et al., 2004). Figure 2 shows the morphology of ZnO powders characterized by SEM. The grain size of both ZnO powders, measured from the difference between the visible grain boundaries, was ~ 200 nm. That is to say the $\text{Zn}(\text{CH}_3\text{COO})_2 \cdot 2\text{H}_2\text{O}$ concentration does not affect the size of ZnO powders in this study. But, the shape of ZnO powder changes from plate-like to spherical shape when the concentration of $\text{Zn}(\text{CH}_3\text{COO})_2 \cdot 2\text{H}_2\text{O}$ was increased. This might be due to a decrease in the mole ratio of NaOH to $\text{Zn}(\text{CH}_3\text{COO})_2 \cdot 2\text{H}_2\text{O}$ in the precursor solution, and an increase of CH_3COO^- species which could adsorb on the (001) positive plane (Suwanboon et al., 2005).

Influence of PVP concentration

In this part, we studied the role of PVP in controlling the size and morphology of ZnO prepared from 0.1 M $\text{Zn}(\text{CH}_3\text{COO})_2 \cdot 2\text{H}_2\text{O}$ precursor solution and the XRD patterns were presented in figure 3. We found that the diffractograms presented a

good crystallinity in the whole ranges of PVP concentrations corresponding to the hexagonal wurtzite structure without any impurity phase as in the first case. The information on lattice parameters and crystallite sizes is summarized in table 1.

Based on the results in table 1, we surmise that PVP played two important roles in this system. First, the PVP promotes the reaction of Zn^{2+} ions with NaOH by generating the OH⁻ groups in solution, favoring more reaction and grain growth. The PVP, secondly, acts as stabilizer or capping agent when the concentration was higher than 1×10^{-4} M. Therefore, the PVP can encapsulate the ZnO particles at higher concentration to suppress the grain growth. In this study, the morphology of ZnO powders was changed from plate-like to a small rod shape when adding the PVP into solution because of the adsorption of protonated PVP species on the (100) negative plane, so the grains can grow in the <001> direction (Caswell *et al.*, 2003). Furthermore, the morphology tended to be monosized at higher PVP concentration, and the grain size is smaller, as shown in figure 4. The grain size of ZnO powders decreased from 148 to 137 and 130 nm at 1×10^{-4} M, 2×10^{-4} M and 3×10^{-4} M PVP, respectively. However, it was observed that there was a difference between the size measurement using XRD and SEM. The reason is well known. In SEM, the grain size was measured by the differences between the visible grain boundaries while in the XRD method, the measurement was confined to the crystalline region that diffracted x-ray coherently. This was a more stringent criterion and led to smaller grain size (Bandyopadhyay *et al.*, 2002).

Considering the ZnO powders obtained from 0.2 M $Zn(CH_3COO)_2 \cdot 2H_2O$ and 0.1 M $Zn(CH_3COO)_2 \cdot 2H_2O$ with 3×10^{-4} M PVP, we found that the ZnO powders from both conditions yielded a similar result in monosized powder. Nevertheless, the grain

size obtained from the condition later is smaller. The shape of ZnO powders obtained from both conditions was unlike as previously mentioned.

Optical properties

Figure 5 shows the absorption spectra of the calcined ZnO powders prepared from 0.1 M $\text{Zn}(\text{CH}_3\text{COO})_2 \cdot 2\text{H}_2\text{O}$ at various PVP concentrations. It was obvious that the ZnO powders performed in a highly transparent mode in visible region. So, it can be used in photodiode application. Based on the absorption spectra, we could estimate the band gap of ZnO powders from the relationship: $(\alpha h\nu)^2 = E_D (h\nu - E_g)$, where α is the optical absorption coefficient, $h\nu$ is the photon energy, E_g is the direct band gap and E_D is a constant (Maensiri et al., 2006). Figure 6 shows a graph of $(\alpha h\nu)^2$ versus $h\nu$ for ZnO powders. The linear portion of the curves when extrapolating to zero was an optical band gap value of ZnO powders. In this study, we obtained the optical band gap of about 3.221, 3.223, 3.225, and 3.229 eV at 0, 1×10^{-4} M, 2×10^{-4} M and 3×10^{-4} M PVP, respectively. The band gap values in this study are larger than the band gap value of ZnO (3.10 eV) in the Maensiri's report (Maensiri et al., 2006). It is clear that the optical band gap increased or shifted to higher energy (blue shift) with increasing PVP concentrations or decreasing the grain size. This blue-shift behavior can explain by the modification of the band structure, i.e., narrowing of both the valence and conduction bands (Mahuya et al., 2004)

Conclusion

The nanocrystalline ZnO powders with the smallest grain size of about 130 nm was successfully synthesized at 0.1 M $\text{Zn}(\text{CH}_3\text{COO})_2 \cdot 2\text{H}_2\text{O}$ and 3×10^{-4} M PVP. So, this powder can be used as photocatalyst. The grain size and crystallite size of ZnO powders that were prepared from PVP-modified $\text{Zn}(\text{CH}_3\text{COO})_2 \cdot 2\text{H}_2\text{O}$ solutions, performed the reduction in grain size when the PVP concentration was increased. The optical band gap of ZnO powders increased from 3.218 to 3.223, 3.225 and 3.229 eV in correspondence with the increase in PVP concentration or decrease in grain size.

Acknowledgement

The author wish to thank the faculty of science, Prince of Songkla University for the funding (seed money project).

References

- Bandyopadhyay, S., Paul, G.K., Roy, R. and Sen, S.K. 2002. Study of structural and electrical properties of grain-boundary modified ZnO films prepared by sol-gel technique, *Mater. Chem. Phys.*, 74 : 83-91.
- Bao, D., Gu, H. and Kuang, A. 1998. Sol-gel-derived c-axis oriented ZnO thin films, *Thin Solid Films.*, 312 : 37-39.
- Cao, G. 2004. *Nanostructures & Nanomaterials: Synthesis, Properties & Application*, Imperial College Press, London, UK, pp. 1-14.
- Caswell, K.K., Bender, C.M. and Murphy, C.J. 2003. Surfactantless wet chemical synthesis of silver wires, *Nano lett.*, 3 : 667-669.
- Huang, Y., Liu, M., Li, Z., Zeng, Y. and Liu, S. 2003. Raman spectroscopy study of ZnO-based ceramic films fabricated by novel sol-gel process, *Mater. Sci. Eng. B.*, 97 : 111-116.
- Lee, J., Lee, D., Lim, D. and Yang, K. 2007. Structural, electrical and optical properties of ZnO:Al films deposited on flexible organic substrates for solar cell applications, *Thin Solid Films.*, 515 : 6094-6098.
- Lee, J.H., Ko, K.H. and Park, B.O. 2003. Electrical and optical properties of ZnO transparent conducting films by the sol-gel method, *J. Cryst. Growth.*, 247 : 119-125.
- Maensiri, S., Laokul, P. and Promarak, V. 2006. Synthesis and optical properties of nanocrystalline ZnO powders by a simple method using zinc acetate dihydrate and poly(vinyl pyrrolidone), *J. Cryst. Growth.*, 289 : 102-106.
- Mahuya, C., Sreetama, D., Chattapadhyay, S., Sarkar, A., Sanyal, D. and Chakrabarti, A. 2004. Grain size dependence of optical properties and positron annihilation parameters in Bi₂O₃ powder, *Nanotech.*, 15 : 1792-1796.

- Majumder, S.B., Jain, M., Dobal, P.S. and Katiyar, R.S. 2003. Investigations on solution derived aluminium doped zinc oxide thin films, *Mater. Sci. Eng. B.*, 103 : 16-25.
- Mohammad, M.T., Hashim, A.A. and Al-Maamory, M.H. 2006. Highly conductive and transparent ZnO thin films prepared by spray pyrolysis technique, *Mater. Chem. Phys.*, 99 : 382-387.
- Pal, U., Garcia, J., Santiago, P., Xiong, G., Ucer, K.B. and Williams, R.T. 2006. Synthesis and optical properties of ZnO nanostructures with different morphologies, *Opt. Mater.*, 29 : 65-69.
- Patil, D.R. and Patil L.A. 2007. Room temperature chlorine gas sensing using surface modified ZnO thick film resistors, *Sensor. Actuat. B-Chem.*, 123 : 546-553.
- Suwanboon, S., Mezy, A., Ravot, D., Tedenac, J.C., Geradin, C and Tichit, D. 2005. Influence of trisodium citrate on controllable ZnO nanoparticles. Proceeding of the 1st Nano-Objets aux Interface: Structure, Organisation et Fonction en Biologie, Chimie et Physique, Montpellier, France, November 22-25, 141-144.
- Tang, H., Yan, M., Ma, X., Zhang, H., Wang, M. and Yang, D. 2006. Gas sensing Behavior of polyvinylpyrrolidone-modified ZnO nanoparticles for trimethylamine, *Sensor. Actuat. B-Chem.*, 113 : 324-328.
- Xu, J., Pan, Q., Shun, Q. and Tian, Z. 2000. Grain size control and gas sensing properties of ZnO gas sensor, *Sensor. Actuat. B-Chem.*, 66 : 277-279.
- Yinghin, L., Yichun, L., Yiying, Z., Youming, L., Dezhen, S. and Xiwu, F. 2006. ZnO hexagonal prisms grown onto p-Si (111) substrate from poly(vinylpyrrolidone) assisted electrochemical assembly. *J. Cryst. Growth.*, 290 : 405-409.

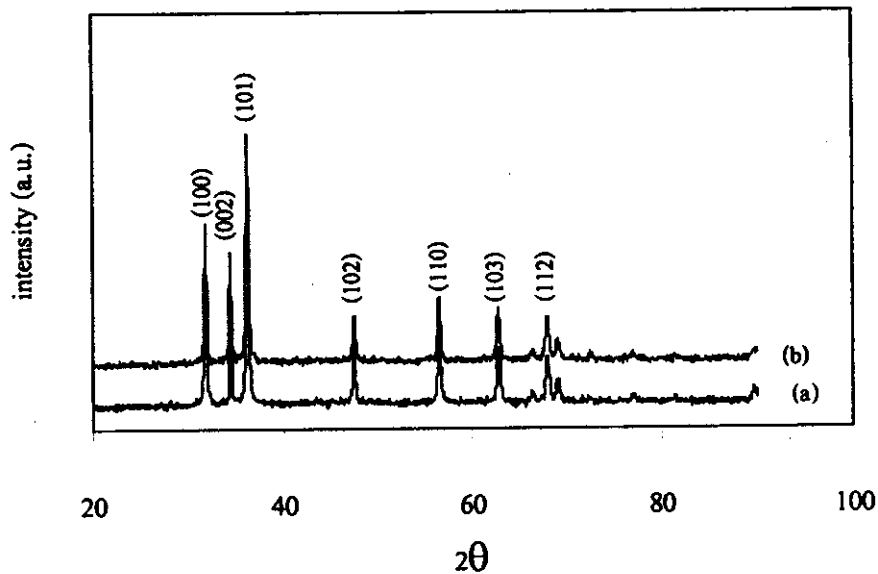


Figure 1. XRD patterns of nanocrystalline ZnO powders prepared from (a) 0.1 M $\text{Zn}(\text{CH}_3\text{COO})_2 \cdot 2\text{H}_2\text{O}$ and (b) 0.2 M $\text{Zn}(\text{CH}_3\text{COO})_2 \cdot 2\text{H}_2\text{O}$.

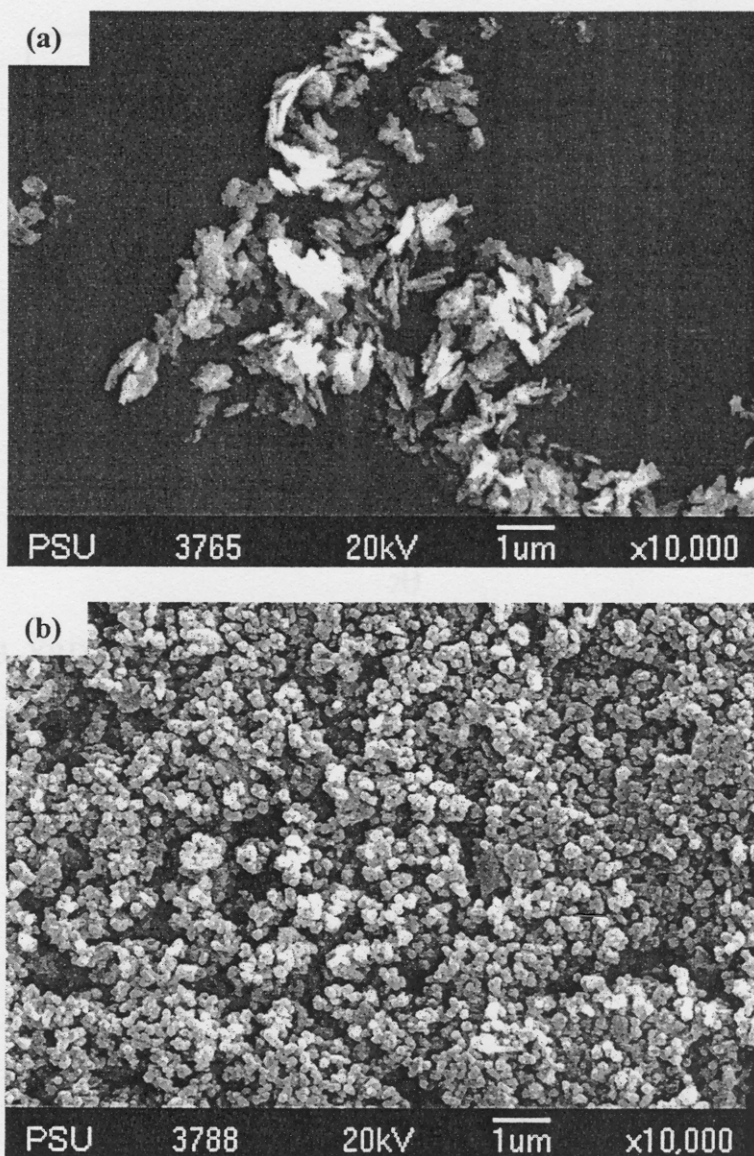


Figure 2. SEM images of nanocrystalline ZnO powders prepared from (a) 0.1M Zn(CH₃COO)₂·2H₂O and (b) 0.2M Zn(CH₃COO)₂·2H₂O

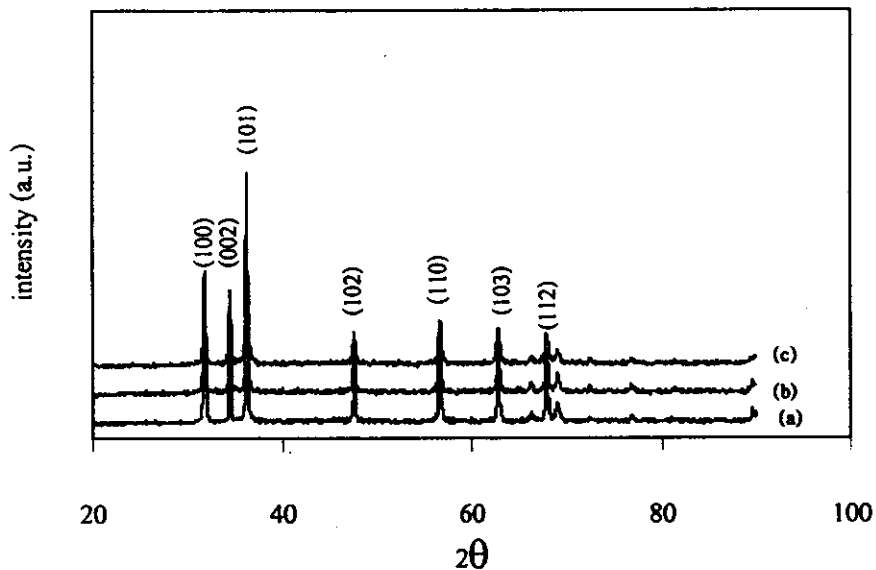


Figure 3. XRD patterns of nanocrystalline ZnO powders prepared from 0.1 M $\text{Zn}(\text{CH}_3\text{COO})_2 \cdot 2\text{H}_2\text{O}$ using PVP as (a) 1×10^{-4} M, (b) 2×10^{-4} M and (c) 3×10^{-4} M, respectively.

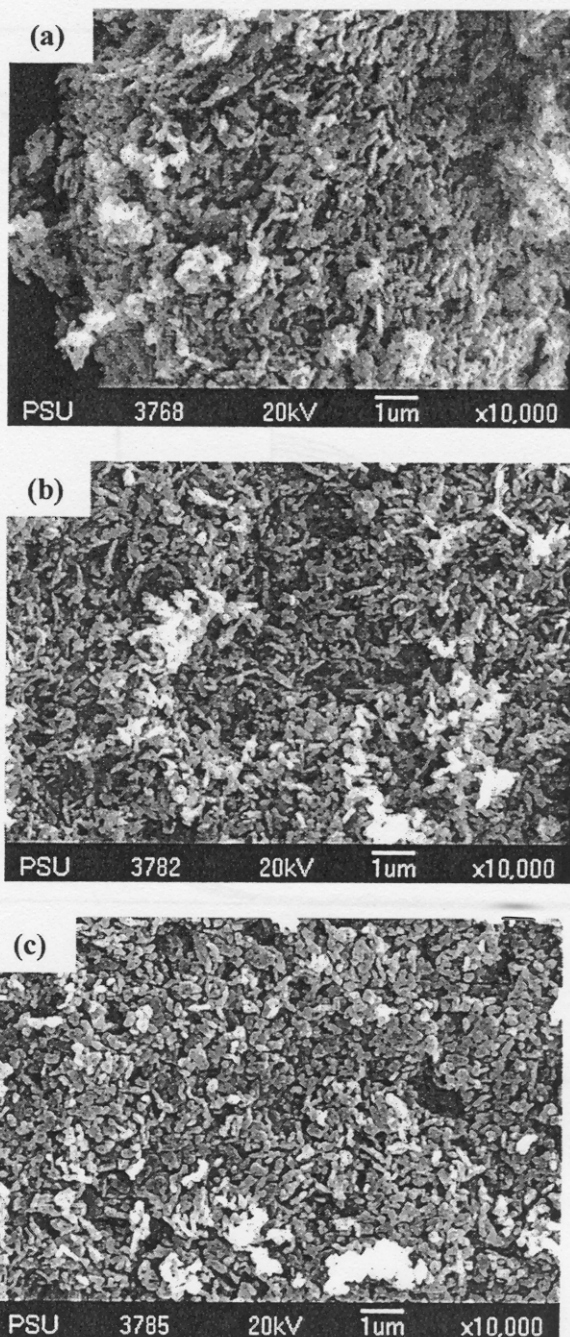


Figure 4. SEM images of nanocrystalline ZnO powders prepared from 0.1M $\text{Zn}(\text{CH}_3\text{COO})_2 \cdot 2\text{H}_2\text{O}$ when using PVP as (a) 1×10^{-4} M, (b) 2×10^{-4} M and (c) 3×10^{-4} M, respectively.

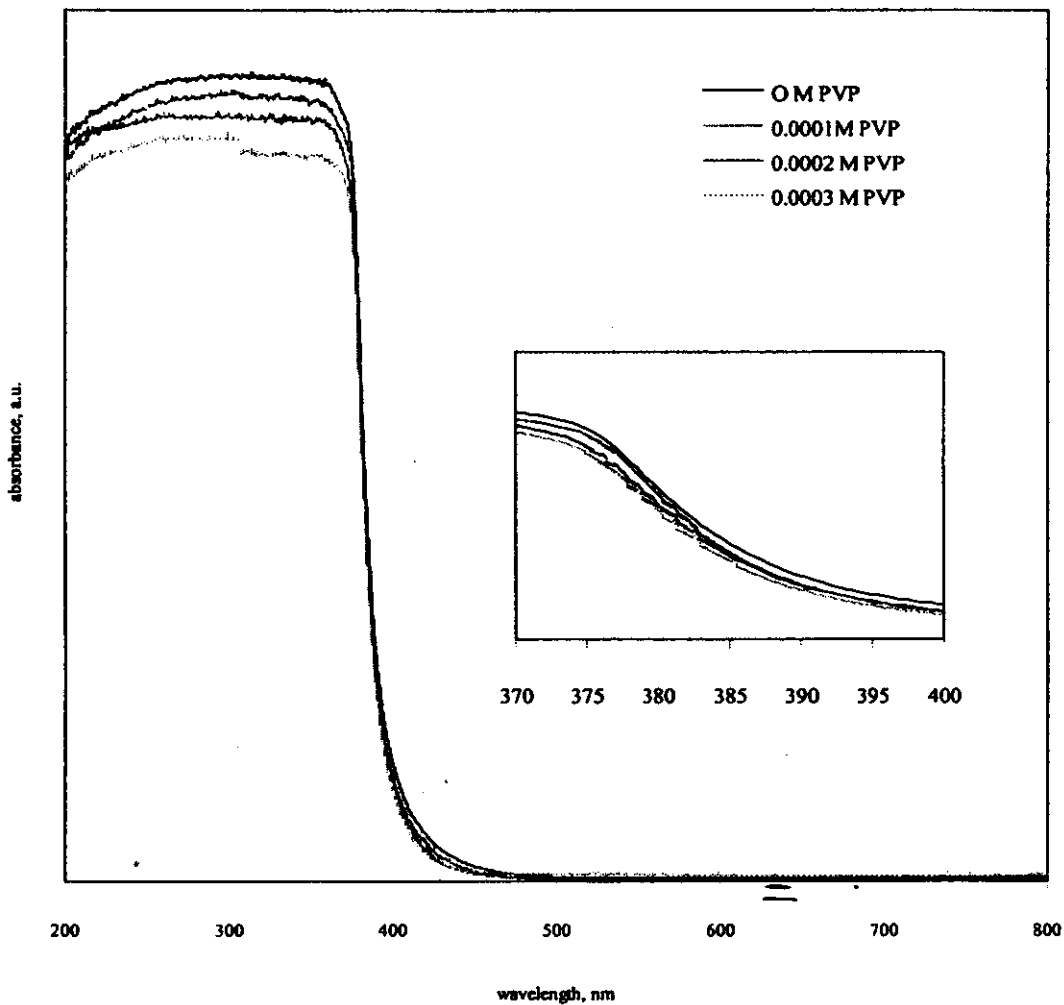


Figure 5. Room temperature optical absorbance spectra of ZnO powders prepared from 0.1 M $\text{Zn}(\text{CH}_3\text{COO})_2 \cdot 2\text{H}_2\text{O}$ when using various PVP concentrations.

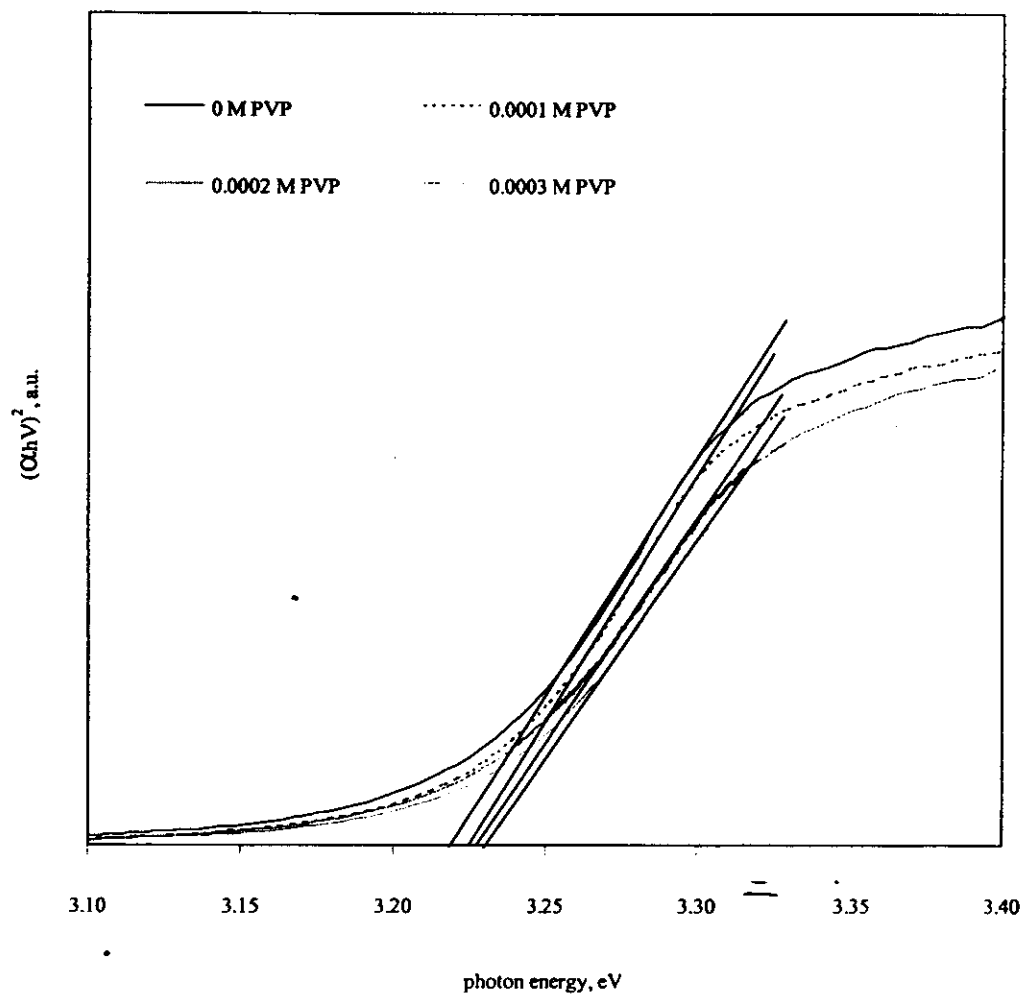


Figure 6. Evolution of the $(\alpha h\nu)^2$ vs. $h\nu$ curves of ZnO powders prepared from 0.1 M $\text{Zn}(\text{CH}_3\text{COO})_2 \cdot 2\text{H}_2\text{O}$ when using various PVP concentrations.

Table 1. The crystallite sizes and lattice parameters estimated from diffraction peaks.

Zn(CH ₃ COO) ₂ ·2H ₂ O (M)	PVP (M)	crystallite size (nm)	Lattice parameter		
			<i>a</i> (nm)	<i>c</i> (nm)	<i>c/a</i>
0.1	1x10 ⁻⁴	55.73 ± 10.97	0.3249	0.5205	1.602
	2x10 ⁻⁴	49.73 ± 6.69	0.3249	0.5205	1.602
	3x10 ⁻⁴	44.76 ± 8.78	0.3249	0.5206	1.602